Chemistry & Biology, Vol. 9, 933–942, August, 2002, ©2002 Elsevier Science Ltd. All rights reserved. PII S1074-5521(02)00187-4

Directed Evolution of High-Affinity Antibody Mimics Using mRNA Display

Lihui Xu, Patti Aha, Ke Gu, Robert G. Kuimelis, Markus Kurz,[2] Terence Lam, Ai Ching Lim, Hongxiang Liu,[3] Peter A. Lohse,[4] Lin Sun, Shawn Weng, Richard W. Wagner, and Dasa Lipovsek[1]
Phylos, Inc.
128 Spring Street
Lexington, Massachusetts 02421

Summary

We constructed a library of $>10^{12}$ unique, covalently coupled mRNA-protein molecules by randomizing three exposed loops of an immunoglobulin-like protein, the tenth fibronectin type III domain (^{10}Fn3). The antibody mimics that bound TNF-α were isolated from the library using mRNA display. Ten rounds of selection produced ^{10}Fn3 variants that bound TNF-α with dissociation constants (K_d) between 1 and 24 nM. After affinity maturation, the lowest K_d measured was 20 pM. Selected antibody mimics were shown to capture TNF-α when immobilized in a protein microarray. ^{10}Fn3-based scaffold libraries and mRNA-display allow the isolation of high-affinity, specific antigen binding proteins; potential applications of such binding proteins include diagnostic protein microarrays and protein therapeutics.

Introduction

Antibodies and other reagents that bind to their targets with high affinity and specificity are in increasing demand as the focus of genomic research expands to include gene products. We designed a library of antibody mimics based on the structure of the tenth fibronectin type III domain (^{10}Fn3), then used the recently-described method of mRNA display [1–8] to select specific affinity reagents of subnanomolar affinity.

Like ribosome display [9, 10], RNA display does not require the transformation of library DNA into a microorganism. As a consequence, the size of the libraries made using these methods is not limited by the transformation efficiency, and libraries with 10^{12}–10^{13} different sequences have been constructed [5, 9, 11]; in contrast, the largest phage library reported to date contains 10^{11} different sequences [12]. RNA display has the added advantage that the association between the mRNA strand and the polypeptide encoded by that mRNA is covalent, which makes possible the selection under stringent conditions, such as at elevated temperature.

Due to the high performance of the natural immune response, the first artificial affinity reagents were based on antibodies and on antibody fragments. The now routine production of polyclonal and monoclonal [13] antibodies in vivo exploits an animal immune system to generate a diverse pool of antibodies and to select those antibodies that bind to the target of interest. In contrast, an in vitro selection of antibodies requires the creation of DNA libraries by cloning the natural immune repertoire of naive or of preimmunized animals [14, 15] or by randomizing the positions in cloned antibody genes that encode the complementarity-determining regions [16, 17]; target binding antibodies are then selected from such libraries under biochemically defined conditions. Due to the challenges associated with the manipulation of proteins that are the size and the complexity of antibodies, most of the in vitro development of antibody-based affinity reagents has focused on antibody fragments such as F_{ab} fragments [18–21], single-chain antibodies [11, 14–16, 22, 23], helix-stabilized antibody fragments [24], and isolated V_H [25–33] and V_L domains [34–36]. In addition, some specific affinity reagents have been selected from peptides [37–42] and from small, globular protein scaffolds not related to antibodies [43–53]. Overall, the scaffolds related to natural antibodies have yielded molecules of higher affinity than did the short peptides and the protein scaffolds not related to antibodies.

We chose the tenth type III domain of human fibronectin (^{10}Fn3), a 94 residue (10 kDa) structural protein [54, 55] with an immunoglobulin-like fold (Figure 1) [56–59] as the antibody-mimic scaffold. The properties that make ^{10}Fn3 a good scaffold candidate include exceptional thermostability (T_m = 90°C) and solubility (>15 mg/ml), high expression level in *E. coli* (50 mg/l), and the lack of disulfide bonds or of unpaired cysteines in its structure [60]. The stability of the wild-type ^{10}Fn3 can be improved further by the removal of unfavorable surface electrostatic interactions [61]. Three of the solvent-accessible loops in ^{10}Fn3, named BC (residues 21–30), DE (residues 51–56), and FG (residues 76–87), are structurally analogous to the V_H complementarity-determining regions (CDR) H1, H2, and H3, respectively (Figure 1). The fact that the sequences of loops BC, DE, and FG are less conserved between different Fn3 domains than is their β sheet framework [57] suggests that a diversity artificially introduced into these three loops may not disturb the overall fold of the domain.

The first report on the use of the ^{10}Fn3 scaffold as an antibody mimic was published by Koide et al. [62]. In that study, a library of 10^8 distinct, ^{10}Fn3-like sequences was made by deleting three residues (82–84) in the FG loop and by randomizing five residues (26–30) in the BC loop and four residues (77–80) in the FG loop. A subsequent phage display selection against immobilized ubiquitin yielded a clone that bound to the target with the IC_{50} of 5 μM, as determined by competition-phage ELISA. The selected ubiquitin binding ^{10}Fn3-like domain showed "broad binding specificity" [62], includ-

[1]Correspondence: dlipovsek@phylos.com
[2]Present address: Archemix Corporation, 1 Hampshire Street, Cambridge, Massachusetts 02139.
[3]Present address: Xencor, Inc., 2585 Nina Street, Pasadena, California 91107.
[4]Present address: Arqule, Inc, 19 Presidential Way, Woburn, Massachusetts 02180.

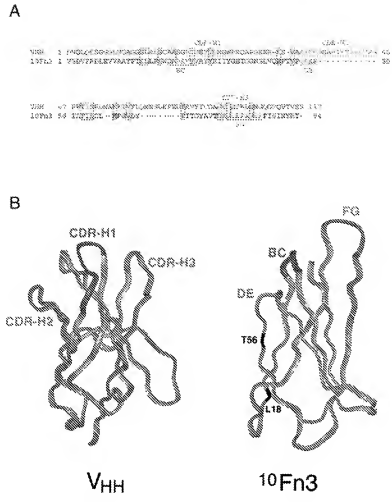

Figure 1. Comparison of the Primary Sequences and of the Tertiary Structures of a Llama V_{HH} Domain and the Wild-Type Human ^{10}Fn3 Domain

A comparison of the primary sequences and of the tertiary structures of a llama V_{HH} domain [70], which is the smallest antibody fragment known to bind to an antigen, and the wild-type, human ^{10}Fn3 domain [56], the scaffold for a new class of antibody mimics. Alignment of primary sequences (A) and structural comparison (B) between these two domains demonstrates that, despite the lack of significant sequence identity, the V_{HH} and the ^{10}Fn3 fold into similar β sheet sandwiches. The disulfide bond between Cys 22 and Cys 92 of the V_{HH} domain is shown in yellow; there are no disulfides in the ^{10}Fn3 domain. The complementarity-determining regions of the V_{HH} and the residues randomized in the ^{10}Fn3-based libraries are shown in color (underlined in the sequence). Blue: CDR-H1 of the llama V_{HH} and residues 23–29 of the ^{10}Fn3 BC loop; green: CDR-H2 of the llama V_{HH} and residues 52–55 of the ^{10}Fn3 DE loop; red: CDR-H3 of the llama V_{HH} and residues 78–87 of the ^{10}Fn3 FG loop. In the sequence alignment, the homologous residues are boxed. The ^{10}Fn3 residues outside the randomized loops that were found to have mutated in approximately 45% of the selected clones are marked in black in the ribbon representation of the ^{10}Fn3 structure.

ing binding to dextran, and dramatically lowered stability and solubility when compared to the wild-type. This study demonstrated the potential utility of the ^{10}Fn3 scaffold, but it left open the question of whether the ^{10}Fn3 structure was robust enough to tolerate the extensive sequence variation required to generate new binding properties [63].

Here we show that the combination of an alternative library design and of the alternative selection method of mRNA display, which allowed the sampling of a larger library, yielded Fn3-based antibody mimics that bound to their target with high specificity and with dissociation constants (K_d) in the pico- to nanomolar range. Furthermore, the selected antibody mimics retained their binding properties when immobilized to create a protein microarray.

Results and Discussion

Library Construction

The ^{10}Fn3-based library was an equimolar mixture of three sublibraries, the first with one randomized loop, FG (ten residues), the second with two randomized loops, BC (seven residues) and FG, and the third with three randomized loops, BC, DE (four residues), and FG. In all, 21 residues were randomized in the library with three randomized loops (Figure 1).

The mixture of the three DNA libraries was transcribed and translated into an RNA-protein fusion library [5], which consisted of 10^{12} members with unique sequences.

Library Diversity

Theoretically, the number of unique amino acid sequences that could appear in the three sublibraries is 10^{13} (20^{10}) for the sublibrary with one randomized loop, 10^{22} (20^{17}) for the sublibrary with two randomized loops, and 10^{27} (20^{23}) for the sublibrary with three randomized loops. It is important to keep in mind that even our library of 10^{12} different molecules sampled only a fraction of such possible sequences.

Another challenge is to translate the sequence diversity of a synthesized DNA library into the functional diversity of the protein library it encodes. Of the 32 codons encoded by the sequence NNS (NNC or NNG), only one is a stop codon. Nevertheless, only 51% ($(31/32)^{23}$) of ^{10}Fn3-like sequences with 21 NNS-encoded positions would be expected to be free of stop codons; the resulting protein diversity would be about half of the original DNA diversity.

To avoid this problem, we synthesized each DNA li-

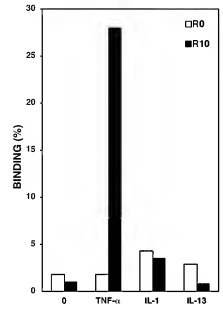

Figure 2. Specificity of Binding of the ^{10}Fn3 Pool Translated from the Original, Randomized Library and from the Pool Obtained after Ten Rounds of Selection for Binding to TNF-α

The library or the PCR product of the elution after R10 was transcribed and translated in vitro, in the presence of ^{35}S-methionine but without forming RNA-protein fusion. The fraction of the resulting free protein bound to underivatized Sepharose, to TNF-α-Sepharose (~10 μM TNF-α in the target-^{10}Fn3 binding mixture), to IL-1α-Sepharose (~30 μM IL-1α), and to IL-13-Sepharose (~50 μM IL-13) is compared. The R10 selected protein pool binds specifically to TNF-α-Sepharose, whereas the R0 library binds at a comparable, low background level to all three immobilized cytokines.

brary in three fragments, each with one randomized region and encoding a C-terminal FLAG peptide. The DNA fragments were transcribed and translated into RNA-polypeptide fusions and affinity purified to recover only the fusions that expressed the FLAG peptide, i.e., that had no internal stop codons. Once the DNA fragments encoding the full-length peptides were assembled into the 94 residue ^{10}Fn3-like domain, the sequence diversity of the assembled sublibraries was determined by the amount of RNA-protein fusion made in vitro, in this case, 2 pmol, which corresponds to 10^{12} full-length molecules. The sequencing of 75 full-length clones (data not shown) from the sublibrary with three randomized loops, before the selection began, confirmed the absence of stop codons.

In Vitro Selection on TNF-α-Sepharose

Significant binding of the RNA-protein fusion pool to TNF-α-Sepharose was detected after nine successive rounds of selection and amplification (R9), when 0.7% of the fusion pool bound to the immobilized target. After an additional round (R10), 7% of the selected RNA-protein fusion pool bound to TNF-α-Sepharose, whereas the binding of the R10 fusion pool to underivatized Sepharose remained under the detection limit of 0.25%. A comparison in binding efficiency of the free protein encoded by the R10 pool to TNF-α and to two other cytokines, IL-1α and IL-13, demonstrated specific binding to TNF-α (Figure 2).

Amino Acid Sequences of Variants Selected on TNF-α-Sepharose

The selected pool of TNF-α binding ^{10}Fn3 variants was found to contain clones with diverse sequences. Thirty-two clones from the R9 pool and 29 clones from the R10 pool were picked at random and sequenced. Thirty-eight of these 61 clones (62%) had unique amino acid sequences and illustrated the remarkable diversity of the target binding ^{10}Fn3-like domains isolated (Table 1A). The fact that 90% of the selected clones originated in the library with all three CDR-like loops randomized suggests that the target may be bound cooperatively by several of these loops. We determined the dissociation constants from TNF-α for all the clones that were represented more than once in R9 and R10 pools, and we found K_d values in the range of 1–24 nM (Table 1A).

The amino acid sequences of the selected clones revealed a number of conserved patterns (Table 1A). The most common motif found in the selected loops was PWA(S/T), which was seen in the DE loop of 54% of the clones; the more loosely defined sequence of PW(A/G) was seen in 67% of the clones. Approximately one-half of the selected clones showed conserved changes in the β sheet core of the protein, which had not been randomized intentionally (Figure 3A); presumably, those changes were due to the mutagenesis by Taq polymerase during PCR amplification or by reverse transcriptase during the synthesis of RNA-protein fusion. Further studies of the recurrent scaffold mutations will determine if these mutations improve stability or ligand binding of the selected ^{10}Fn3-like domains.

In Vitro Selection in Solution and Affinity Maturation

Due to the diversity of the selected R10 pool, four additional rounds of selection (R11–R14) were conducted under increased selection pressure in order to isolate the highest-affinity molecules in the pool. The selection rounds R11–R14 were performed in solution, using biotinylated TNF-α at the concentration of 0.5 nM, which was approximately 10^4-fold lower than the concentration of TNF-α-Sepharose during R1–R10. In addition, the selection was performed at an elevated temperature (30°C versus 4°C) and with extended washes of the bound complexes. Twenty-two clones from the R14 pool were chosen at random and sequenced and were found to represent 15 different loop sequences (Table 1B). The lowest K_d values measured for these sequences, 90 pM (for clone T14.25) and 110 pM (for clone T14.20) were an order of magnitude lower than those observed in the R9 and R10 pools. A parallel strategy incorporated error-prone PCR into the amplification of DNA between rounds of selection [64]. The diverse DNA pool from R8 of the TNF-α-Sepharose selection was subjected to two rounds of selection in solution with mutagenesis at the frequency of 0.8%–4.8% (M9) and of 0.8%–2.4% (M10), then to two more rounds of selection without the mutagenesis (M11–M12). The 20 M12 clones tested showed tighter binding to TNF-α than had the clones selected using the two earlier selection protocols (Table 1C); the tightest binding of TNF-α was seen in M12.04, which had the observed K_d of 20 pM. The M12.04 sequence contains a 6 residue deletion in the FG loop as well as

Table 1. Loop Sequences and Binding Properties of ^{10}Fn3-Derived Protein Pools and Variants

Clone	Number	BC	DE	FG	K_d (nM)
Wild-type	0	DAPAVTV	GSKS	GRGDSPASSK	>1000
R0 pool	-	XXXXXXX	XXXX	XXXXXXXXXX	>1000
A R09 pool[a]	-	XXXXXXX	XXXX	XXXXXXXXXX	3 ± 2
R10 pool[a]	-	XXXXXXX	XXXX	XXXXXXXXXX	2 ± 1
T09.07	2	ASPPNWC	PWAT	EYLFEWNMTQ	1 ± 0.5
T10.06	3	NRSGLQS	PWAS	DKSDTYKYDD	2 ± 0.5
T09.12	3	RPTSNPP	PWAS	AQTGHHLHDK	4 ± 2
10.15	2	HTERSFP	PWGS	EHYRDTGTGH	4 ± 2
T09.05	2	TTRHSPV	PWAT	MPTNWRFPHR	17 ± 6
T09.03	2	RPNPRLS	GLFS	PKETSNIFIA	13 ± 6
T10.33	2	SPPNDAH	GSKS	DQQSYTYYSN	17 ± 1
T09.34	2	RTPASPH	LLWP	PTHMLKPQSM	18 ± 2
T09.14	2	YRHTYRD	PWAT	DTGYDVHTKR	24 ± 2
T09.33	5	NRSGLQS	PWAS	SNVGRLDTRY	PPT
B R14 pool[a]	-	XXXXXXX	XXXX	XXXXXXXXXX	0.4 ± 0.2
T14.25	1	DTHNAYN	HPEV	NHHMPLRIFG	0.09 ± 0.02
T14.20	1	RNIYPIA	PWAS	DKSDTYKYDD	0.11 ± 0.03
T14.24	1	NRSGLQC	PWAS	DQRDTYKYDD	0.32 ± 0.02
T14.22	1	RPGRTYS	PWAN	FPTGYPLTEM	0.4 ± 0.2
T14.10	1	RPGRTYS	PWAN	FPPGYPLTEM	0.5 ± 0.2
T14.02	1	MTPHNHV	TGNA	PHHGHFDLEP	0.5 ± 0.1
T14.08	1	TRTNAST	NFWW	SPDETSAYSE	1.4 ± 0.4
T10.06	8	NRSGLQS	PWAS	DKSDTYKYDD	2 ± 0.5
T14.21	1	RPGRTYS	PWAN	YTHSTPMQDE	7 ± 2
T09.34	1	RTPASPH	LLWP	PTHMLKPQSM	18 ± 2
T14.03	1	TRTNANT	NNPP	PDGSRHMLTK	>1000
T14.01	1	DNSRPNT	PWGS	TSECHKLSST	PPT
T14.11	1	NPNRSFA	PWAS	AQTGHHLHDK	PPT
C M12 pool[c]	-	XXXXXXX	XXXX	XXXXXXXXXX	0.4 ± 0.1
M12.04	1	SMTPNWP	PWAS	HRDT	0.02 ± 0.01
T14.25	1	DTHNAYN	HPEV	IHHMPLRIFG	0.09 ± 0.02
M12.18	1	ASPPMW	PWAT	DESWSDRSMD	0.2 ± 0.1
M12.26	1	RPPADLN	PWGT	HRDT	0.2 ± 0.1
M12.12	3	EQSPTYG	GSKS	IEKDRIPLFG	0.2 ± 0.05
M12.13	1	RPGRTYS	PWAN	FPPGYPLTEM	0.3 ± 0.2
M12.16	1	RPGRTYS	PWAS	DKSGTYRYDD	0.3 ± 0.05
M12.21	1	YRHTYRD	PWAT	DAGYDVHTKR	0.3 ± 0.1
M12.23	1	RTMPVTA	PWAS	SATPSRPNVH	0.3 ± 0.1
M12.09	2	RPGRAYS	PWAN	FPPRYLTEM	0.4 ± 0.1
M12.05	1	SPPNDAH	GSKS	DQQSYTYYSN	0.5 ± 0.2
M12.08	1	II	APKA	SHRNHFHVET	0.6 ± 0.05
M12.19	1	RNNQYTP	ELNP	QNGTPRVIYG	0.6 ± 0.2
M12.22	1	RPASNPA	PWAS	AQTGHRLHDK	0.7 ± 0.2
M12.24	2	NRSGLQS	PWAS	PNVGRLDTRY	1.3 ± 0.7
M12.01	2	NRSGLQS	PWAS	DESDTYKYDD	1.6 ± 0.2
M12.14	1	THSNVPA	PWAS	LYTGNHRPEH	1.7 ± 0.4
M12.07	1	RSGNRTT	PWAT	THNSTAQPEY	4 ± 2
M12.25	1	NRSGLQS	PWAS	SNVGRLDTRY	>1000
M12.15	1	RNAKDPG	PWGT	ATNPGPTQHR	PPT

The first two digits of the name of the clone show the round of selection from which the clone was derived. "Number" indicates the number of clones with the amino acid residue sequence in loops BC, DE, and FG that is identical to the clone listed. Since no systematic difference was observed between the R9 and R10 pools, the entry in Table 1A is the combined number of clones isolated from these two pools. The amino acid residue sequence of loop BC, DE, or FG in the specified clone is shown. Dissociation constant (K_d) for the binding of the free protein form of the specific ^{10}Fn3 clone to trimeric TNF-α, at room temperature, is shown. The values reported and the associated errors were derived from 2–4 independent measurements. PPT indicates protein sample was not soluble under conditions used for K_d determination.

[a] After nine (R9) and after ten (R10) rounds of selection using TNF-α-Sepharose.

[b] After four rounds of selection starting with the R10 pool and using biotin-TNF-α (R14).

[c] After two selection rounds with error-prone PCR, followed by two selection rounds with standard Taq PCR, starting with the R8 pool and using biotin-TNF-α (M12). Wild-type ^{10}Fn3 sequences are bold.

the frequently selected PWAS tetrapeptide in the DE loop. Two other high-affinity TNF-α binding variants that evolved using error-prone PCR, M12.26 and M12.08, resulted from major deletions in the randomized loops (six residues in the FG loop and five residues in the BC loop, respectively); in contrast, no deletions were found in any of the characterized variants derived without error-prone PCR. These results demonstrate that low-level, random mutagenesis late in a selection can improve both the binding affinity of selected antibody mimics (20 pM versus 90 pM) and the speed with which they can be selected (12 rounds versus 14 rounds).

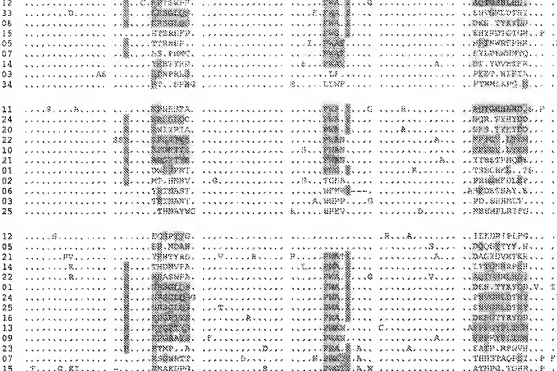

Figure 3. Alignment of the Amino Acid Residue Sequences of the Wild-Type ^{10}Fn3 and of the Selected Fn3 Variants

(A) After nine (R9) and after ten (R10) rounds of selection using TNF-α-Sepharose.

(B) After four rounds of selection starting with the R10 pool and using biotin-TNF-α (R14).

(C) After two selection rounds with error-prone PCR, followed by two selection rounds with standard Taq PCR, starting with the R8 pool and using biotin-TNF-α (M12).

The residues identical to those of wild-type ^{10}Fn3 are represented by dots, deletions are represented by dashes, and the amino acid residues different from the corresponding wild-type residues are identified by one-letter code. The variable-loop sequences that appeared in several different clones are highlighted, as are the changes at the two most variable positions outside the randomized loops, positions #18 and #56.

Biophysical State of Fn3-Based Antibody Mimics

To confirm that the selected antibody mimics fold into a three-dimensional structure, the wild-type human ^{10}Fn3 and two representative variants, T09.07 and M12.21, were expressed in *E. coli*, purified using the hexahistidine affinity tag, and incubated with thermolysin at temperatures between 4°C and 50°C. As expected for a highly thermostable protein, wild-type ^{10}Fn3 resisted proteolysis throughout the temperature range tested, suggesting that the sample was completely folded under those conditions. In contrast, a fraction of the protein in T09.07 and M12.21 samples was found to be sensitive to proteolysis at 37°C and 25°C, respectively (Figure 4). Approximately 50% of the T09.07 domain resisted the protease after a 15 min incubation of 42°C, and approximately 40% of M12.21 resisted the protease after such an incubation at 30°C. This finding demonstrates that, whereas the two variants are less stable than the wild-type ^{10}Fn3, they are predominantly folded at room temperature, the temperature at which their binding was characterized; in other words, the selected loop sequences bind their targets in the context of a folded domain.

In addition, analytical gel filtration showed that the apparent molecular weight of purified, soluble wild-type ^{10}Fn3, T09.07, and M12.21 at 0.1–1 mg/ml is consistent with the variants being monomeric. Consequently, the Fn3 samples used to determine their K_d, which were three orders of magnitude more dilute, were likely to interact with TNF-α as monomers.

Fn3-Based Antibody Mimics in Protein Microarrays

To demonstrate the utility and the specificity of ^{10}Fn3-based antibody mimics, we tested their activity when immobilized onto a solid surface. In these studies, we included a ^{10}Fn3 variant that binds to leptin, clone L9.20, which had been selected from the same ^{10}Fn3-based library and under similar selection conditions as the

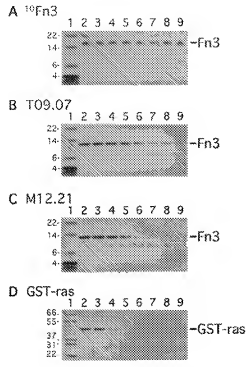

Figure 4. Sensitivity of Selected Domains to Thermolysin

Sensitivity to thermolysin with increasing temperature for (A) wild-type, human ^{10}Fn3, (B) T09.07, (C) variant M12.21, and (D) unfolded control (ras-derived peptide [1–189] fused to GST [GST-ras]). Lane 1: molecular weight standards, labeled in kDa. Lanes 2–9: samples after 15 min incubation at increasing temperature, with thermolysin at 20 ng/ml (T) or without thermolysin (0). Lane 2, 4°C, 0; lane 3, 25°C, 0; lane 4, 4°C, T; lane 5, 25°C, T; lane 6, 30°C, T; lane 7, 37°C, T; lane 8, 42°C, T; lane 9, 50°C, T. The arrow on the right points at the position of full-length Fn3 or full-length GST-ras. No proteolysis of the wild-type was observed between 4°C and 50°C, but the selected variants were degraded, with about a half of the full-length domain gone at 42°C for T09.07 and at 30°C for M12.21. Most of the control protein, the fusion of glutathion-S-transferase with an unstructured, ras-derived peptide (GST-ras), was degraded already when exposed to thermolysin at 4°C.

TNF-α binding variants (L.S., A. Kovtun, Y. Chen, H. Gao, P. Amersdorfer, B. Kreider, and R.W.W., unpublished data) and which had the K_d for leptin of 0.8 nM.

To generate the microarrays, a Watson-Crick immobilization scheme was used to attach the ^{10}Fn3 variants to a glass surface [65]. In this method, mRNA-protein fusions were prepared using DNA linkers with sequences that were clone specific. This allowed the antibody-mimic fusions to self-assemble onto an array spotted with the capture probe complementary to their respective DNA linkers. Following RNase A digestion of the RNA portion of the fusion, the resulting DNA-tagged ^{10}Fn3 variants were allowed to hybridize to the array, thereby immobilizing the antibody mimics via their carboxyl termini and exposing their target binding loops to solution.

In the first test, the binding properties of wild-type ^{10}Fn3, of T09.12 (a ^{10}Fn3 variant selected for binding to TNF-α), and of L09.20 (a ^{10}Fn3 variant selected for binding to leptin) were compared when these three domains were immobilized on a microarray. Each of the antibody

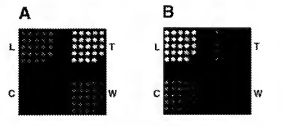

Figure 5. Specific Capture of TNF-α and of Leptin by an Antibody Mimic Immobilized on a Solid Surface

Two identical microarrays were constructed by immobilizing DNA-puromycin-Fn3 constructs on a glass surface that contained a TNF-α binding Fn3 variant, T09.12 (T), a leptin binding Fn3 variant, L09.20 (L), and wild-type human ^{10}Fn3 (W). Capture oligonucleotides complementary to the DNA linker attached to the Fn3 protein were used to direct the constructs to specific locations. The fourth set of features (C) was created by spotting onto the chip an oligonucleotide not complementary to any of the DNA sequences present in the fusions. To examine the binding properties of the immobilized Fn3, the first fusion microarray (A) was exposed to 100 nM biotinylated TNF-α, and the second microarray (B) to 100 nM biotinylated leptin. Next, bound target was visualized using a Cy3-labeled anti-biotin monoclonal antibody.

mimics was prepared as an ^{35}S-labeled RNA-protein fusion, digested with RNase, and allowed to self-assemble into the predetermined position on a glass slide. The immobilization onto the array was confirmed by radioactive imaging of the ^{35}S-labeled, protein portion of the fusion (data not shown). After an incubation with the target proteins, T09.12 and L09.20 were found to bind their respective targets, but not to bind each other's targets. As expected, the wild-type ^{10}Fn3 bound neither TNF-α nor leptin (Figure 5).

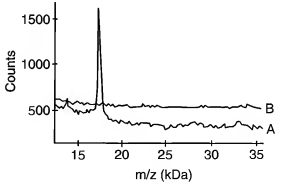

Figure 6. Specific Capture of TNF-α from a Biological Fluid by an Antibody Mimic Immobilized on a Solid Surface

DNA-puromycin-Fn3 constructs of the T09.12 variant (A) and of the wild-type ^{10}Fn3 (B) were hybridized to a glass cover slip arrayed with an immobilized oligonucleotide complementary to the DNA linker. After washing, the surfaces were exposed to TNF-α (1.5 mg/ml, in 90% v/v PBS, with or without 10% fetal bovine serum), the dried chip was spotted with MALDI matrix (200 μm feature size), and a single feature was analyzed with a Voyager DE MALDI-TOF mass spectrometer (PerSeptive Biosystems). A signal at 17.4 kDa, which corresponds to the expected molecular mass of monomeric TNF-α, was detected on the feature that contained T09.12 protein (A), but not on the feature that contained wild-type ^{10}Fn3 (B). This demonstrates that the Fn3 variant selected for the binding of TNF-α can capture its target specifically from the background of 10% FBS.

In the second test, the TNF-α binding antibody mimic T09.12 was immobilized in the same fashion onto a glass slide coated with its capture oligonucleotide. Following an incubation with TNF-α and subsequent printing with matrix material, the features were analyzed for the presence of TNF-α using mass spectroscopy. T09.12 was shown to capture TNF-α when this target protein was spiked into either PBS buffer or into PBS with 10% fetal bovine serum (FBS); no other predominant proteins, such as those present in bovine serum, were detected (Figure 6).

Together, the results of these two experiments demonstrate that the inherent specificity of the ^{10}Fn3-based antibody mimics was preserved when these mimics were immobilized on a solid surface.

Conclusion

The large library size made possible by the in vitro mRNA display technology allowed us to randomize all three CDR-like loops of ^{10}Fn3 and to sample 10^{4}-fold more sequences than was possible in the phage-display selection reported by Koide et al. [62]. Most likely, these improvements in library construction and in selection methodology were the major factors that contributed to the following improvements in the ^{10}Fn3-based antibody mimics: (1) the higher affinity (20 pM [K_d] versus 5 μM [IC_{50}] [62]), (2) the increased specificity, and (3) the larger population of variants with comparable binding properties (100 versus 1 [62]).

This work introduces the ^{10}Fn3 scaffold as a viable alternative both to antibody fragments and to single-chain antibodies in the development of high-affinity, specific binding reagents. For example, two recent single-chain antibody selections, which used the Human Combinatorial Antibody Library and ribosome display, yielded antibody fragments against bovine insulin [11] and against guanine-quadruplex DNA [66] with K_d as low as 80 pM and 125 pM, respectively, affinities close to that described in this paper. Furthermore, ^{10}Fn3-based antibody mimics may be preferable to antibodies in applications that favor small domain size or the absence of disulfide bridges.

One potential application of ^{10}Fn3-based antibody mimics is in diagnostic protein microarrays [67–69], where a large series of specific, ^{10}Fn3-based antibody mimics will be immobilized on a solid surface. Antibody mimics on such a protein microarray could be used to capture, and thus to identify and quantify, their respective antigens from complex biological fluids. In an effort to develop a protein capture array, we have selected ^{10}Fn3-based antibody mimics against a range of cytokines and cytokine receptors with affinity and specificity similar to that described here (L.S., A. Kovtun, Y. Chen, H. Gao, P. Amersdorfer, B. Kreider, and R.W.W., unpublished data). The ability of two such antibody mimics against different cytokines to capture their targets specifically when immobilized on a glass slide (Figure 5) increases our confidence in the feasibility of diagnostic protein arrays based on ^{10}Fn3-like antibody mimics.

Significance

This work introduces the ^{10}Fn3 scaffold, a 94 residue domain with an immunoglobulin-like fold as an alternative to antibody fragments and to single-chain antibodies in the development of subnanomolar, specific binding reagents. The ^{10}Fn3-based antibody mimics may offer advantages over antibodies for applications that favor their small size, their stability under reducing conditions, and their ease of production in *E. coli*. The mRNA display technology used here to select the ^{10}Fn3 variants that bind TNF-α with 20 pM–24 nM affinity allows the creation of libraries of over 10^{12} different sequences, which increases the likelihood that domains with desired binding properties will be found. Future libraries based on different types of β-sandwich scaffolds will allow the selection of antibody mimics with the wide range of properties required in research, diagnostic, and therapeutic applications.

Experimental Procedures

Library Construction

Each library was constructed from three segments prepared either by PCR of the ^{10}Fn3 clone (for wild-type segments), or by DNA synthesis (for segments comprising random sequences; Oligos, Etc.). Each segment that included a randomized loop was made from an overlapping pair of oligonucleotides, one of which contained the randomized region. The randomized positions were encoded by NNS, where N represents an equimolar mixture of all four nucleotides and S represents the equimolar mixture of G and C. For randomized BC, DE, or FG loops, positions encoding amino acid residues 23–29, 52–55, or 77–86, respectively, were substituted with NNS. In addition to the ^{10}Fn3-based sequences, these gene fragments contained 5′ Tobacco Mosaic Virus (TMV) untranslated region and T7 promoter, as well as the sequences encoding N-terminal hexahistidine and C-terminal FLAG-epitope purification tags [5], and 5′ and 3′ *Ear I* restriction endonuclease recognition sites. Each pair of oligonucleotides was annealed and extended using Klenow (NEB) into a double-stranded DNA fragment, which was transcribed in vitro (T7-MEGAshortscript™, Ambion). The resulting mRNA was ligated to the puromycin-containing DNA-polyethylene glycol (PEG) linker (5′-dA_{18}PEG2dCdCPur) using DNA ligase (Promega) and a DNA splint oligonucleotide. The in vitro translation of the ligated mRNA in rabbit reticulocyte lysate (Ambion), in the presence of ^{35}S-methionine, resulted in an mRNA-peptide fusion. The fusion was purified by Oligo(dT)-Cellulose (Type 7, Amersham Pharmacia) and reverse transcribed (Superscript™ II, GIBCO) to generate a DNA strand complementary to the fusion mRNA. Full-length DNA/mRNA-peptide molecules were purified by affinity chromatography first on Ni-NTA agarose (Qiagen) and then on M2 Anti-Flag® Agarose (Sigma). The genetic information encoding each purified fragment was amplified by PCR, which removed the His_6 tag on the N terminus of the molecule, then cleaved by *EarI* (NEB) and ligated to the appropriate randomized or wild-type fragments of DNA to make the three libraries. Finally, 2 pmol of each DNA library were combined to prepare the ^{10}Fn3-based, master library. The DNA master library was processed into a DNA/mRNA-protein library following the procedure described for the individual fragments; no affinity purification was used in rounds one and two, whereas purification on M2-agarose was used in rounds three to ten. Forty picomoles of DNA/mRNA-protein fusion library molecules, the equivalent of 20 copies of 4×10^{12} different sequences, were recovered, then subjected to the first round (R1) of the selection.

In Vitro Selection on TNF-α-Sepharose

TNF-α (PeproTech) was immobilized on Epoxy-Activated Sepharose™ 6B (Amersham Pharmacia) and blocked in Binding Buffer (R1–R6: 50 mM HEPES [pH 7.4], 0.02% Triton, 0.1 mg/ml sheared salmon sperm DNA [Ambion]; R7–R10: as in R1–R6, with additional 1 mg/ml BSA [Sigma]).

In the first step of a selection, the DNA/mRNA-protein library (R1: 40 pmol, R2: 24 pmol, R3–R10: 0.1–2 pmol) was precleared with Epoxy-Sepharose that had been subjected to the derivatization pro-

cedure in the absence of TNF-α. The supernatant was incubated with TNF-α–Sepharose, which was then washed 3× with binding buffer, eluted with 0.1 M KOH, and neutralized. The next round of selection began with PCR amplification of the eluted DNA, followed by transcription, translation, and reverse-transcription into an enriched, DNA/mRNA-protein pool.

In Vitro Selection in Solution

Precleared, 0.1 nM DNA/mRNA-^{18}Fn3 fusion library was incubated with 0.5 nM biotinylated TNF-α in binding buffer (50 mM HEPES [pH 7.4], 0.02% Triton, 0.1 mg/ml sheared salmon sperm DNA [Ambion]; 1 mg/ml BSA [Sigma]), then the complex was captured with Dynabeads® M-280 Streptavidin paramagnetic beads (Dynal) that had been preblocked in the binding buffer. The beads were washed with binding buffer for 1, 15, and 30 min in the case of R11 and R12, or for 1 min, followed by nine 10 min washes, in the case of R13–R14. DNA was eluted with KOH and used to make the next generation DNA/mRNA-^{18}Fn3 fusion library. Round 14 differed from R11–R13 in that the selection was performed at 30°C rather than at 4°C and in the presence of additional 150 mM NaCl.

The DNA pool eluted after R8 was amplified using error-prone PCR, with the pool divided into seven equal parts and mutagenized at the target frequency of 0.8%, 1.6%, 2.4%, 3.2%, 4.0%, and 4.8% using the Diversify™ PCR Random Mutagenesis Kit (Clontech). The seven PCR reactions were combined, and DNA/RNA-protein fusion was made from the mixture and subjected to a round of selection in solution. Before the second mutagenic round, M10, error-prone PCR was performed in three separate reactions, at 0.8%, 1.6%, and 2.4%. The two remaining rounds, M11 and M12, were performed using standard Taq PCR. Except for the mutagenesis, the selection conditions for M9–M12 were the same as for R11–R14.

The leptin binding Fn3 variant L09.20, which was used to examine the specificity of TNF-α binding variants in protein microarrays, was selected in solution, using biotinylated leptin and a protocol similar to the one described above. No error-prone PCR was used in the leptin selection, and the concentration of biotinylated leptin was decreased gradually from 250 nM in R1 to 14 nM in R9 (L.S., A. Kovtun, Y. Chen, H. Gao, P. Amersdorfer, B. Kreider, and R.W.W., unpublished data).

Determination of Dissociation Constants

For R9, R10, R14, and M12 pools, as well as for each characterized clone derived from these pools, 11 samples of 0.25 nM, in vitro-translated, ^{35}S-methionine-labeled protein were incubated with biotinylated TNF-α at concentrations between 17 pM and 25 nM, in 200 μl 10 mM HEPES (pH 7.4), 150 mM NaCl, 1% BSA, 0.02% Triton, for 1 hr at room temperature. Subsequently, each sample was loaded on a presoaked, SAM2R Biotin Capture Membrane (Promega) using a 96-well, Easy-Titer™ ELIFA system (Pierce). Under vacuum, each spot was washed with 200 μl of HBS (pH 7.4), 1% BSA, 0.05% Triton; next, the entire membrane was rinsed in the same buffer and air-dried. The membrane was exposed with a Storage Phosphor Screen (Molecular Dynamics) overnight, and the intensities of the resulting individual spots were quantified using a STORM 860 phosphorimager with the ImageQuaNT densitometry program (Molecular Dynamics). The K_d of the complex was determined by fitting the data to the unsimplified equilibrium binding equation $S = S_{max} / B_t \{[B_t + T_t + K_d] / 2 - \sqrt{([B_t + T_t + K_d]^2 / 2) - B_t T_t}\} + NS$, where S is ^{35}S signal, B_t is the input concentration of the target binding Fn3 domain, T_t is the input concentration of the target, K_d is the dissociation constant, and NS is the signal from nonspecific background binding. The program KaleidaGraph (Synergy Software) was used to fit the data to the equation and to calculate K_d values.

Expression and Biophysical State of Fn3-Based Antibody Mimics

Antibody mimics were expressed in *E. coli* BL21(DE3) pLysS (Invitrogen) from pET-based vectors (Novagen; pET25 for T09.07, pET9a for M12.21 and for the wild-type). The sequences cloned onto the C terminus of the clones for detection, purification, and attachment to the solid phase were HHHHHHGSGSKKKK for T09.07 and for M12.21 and LEGAPVPYPDPLEPRHHHHHHGSGSKKKK for the wild-type ^{18}Fn3. Five hundred milliliters of LB with the appropriate antibiotic (carbenicillin for T09.07, kanamycin for M12.21 and for wild-type ^{18}Fn3) were inoculated with 10 ml of an overnight culture and grown at 25°C, with shaking at 275 rpm, to OD_{600} of 0.6–0.8. The culture was induced with 0.5 mM IPTG, shaken for another 16 hr, and harvested by centrifugation at 3000 × g. The pelleted bacteria were douncе-homogenized and freeze-thawed in 50 ml of lysis buffer (50 mM phosphate [pH 8.0], 0.5 M NaCl, 5% glycerol, 10 mM CHAPS, 25 mM imidazole, 1 mM PMSF, 25 μg/ml DNase I [Roche], 2 μg/ml aprotonin [Roche], and 1 EDTA-free Protease Inhibitor Cocktail tablet [Roche]). After the addition of another 25 μg/ml of DNase and 1 mg/ml of lysozyme, the mixture was incubated at room temperature for 15 min, then centrifuged for 30 min at 27,000 × g. The supernatant was incubated for 30 min at 4°C with 1 ml of TALON™ Superflow™ Metal Affinity Resin (CLONTECH) prewashed with 4 × 10 ml of wash buffer (50 mM phosphate [pH 8.0], 0.5 M NaCl, 5% glycerol, 5 mM CHAPS, 25 mM imidazole). The His-tagged Fn3 domains were eluted with 12 × 0.5 ml of 50 mM HEPES (pH 7.4), 150 mM NaCl, 5 mM CHAPS, 50 mM EDTA, 1 mM PMSF, 2 μg/ml aprotonin, and 1 EDTA-free Protease Inhibitor Cocktail tablet, concentrated to 1 ml in CentriPrep-10 (Millipore), and exchanged into HBS using a NAP-10 column (Amersham Pharmacia). The final yield was 1.8 mg/l for T09.07, 3.6 mg/l for M12.21, and 18 mg/l for the wild-type ^{18}Fn3.

Protease digestion of 2 μg samples of the purified Fn3-based domain or of the control peptide (Ras#1-189) fused to the C terminus of glutathione-S-transferase (GST-ras) was performed in 30 μl of HBS, 5 mM $MgCl_2$, 1 mM DTT, with 20 ng of thermolysin (Sigma-Aldrich) in water baths maintained at 4°C, 25°C, 30°C, 37°C, 42°C, and 50°C. After a 15 min incubation, each reaction was stopped by the addition of 10 μl of 4× SDS-PAGE buffer. Twenty microliters of each sample was separated on an SDS-PAGE gel (Novex; 16% Tricine for selected Fn3-like domains, and 10%–20% Tris-Glycine for GST-ras). The resulting gels were destained, and the relative amount of protein in each band was quantified using a Chemilmager™ 4400 Low Light Imagine System and AlphaEase™ software (Alpha Innotech Corporation). The decrease in intensity of the band containing full-length Fn3 was used to monitor the extent of proteolytic degradation.

The aggregation state of purified wild-type ^{18}Fn3, of T09.07, and of M12.21 were compared using size-exclusion chromatography on a Waters™ 600E Multisolvent Delivery system, with a 7.8 mm × 15.0 cm (5 μm) QC PAK GFC 200 column (Toso Haas). Ten microliters of each sample at 0.1–1.2 mg/ml was loaded onto the column and separated in HBS, at 1 ml/min, for 20 min. Protein absorption at 280 nm was monitored, and the retention time of the major peak, which corresponded to the protein of the highest molecular weight species present in the sample, was compared to the retention time of molecular weight standards. The retention times of wild-type ^{18}Fn3, of the T09.07 variant, and of the M12.21 variant were found to be 6.33, 6.29, and 6.28 min, respectively. These values fall between the retention times of the molecular weight standards ribonuclease A (13.7 kDa) and aprotonin (6.5 kDa), which are 6.01 and 9.08 min, respectively, suggesting that the molecular weights of the Fn3 domains studied are between 7 and 14 kDa.

Construction of Antibody-Mimic Protein Arrays

Each of the antibody mimics to be immobilized was prepared in the form of an mRNA-Fn3 fusion as described above, but with specific DNA-puromycin linkers to encode the identity of the Fn3 variant in the fusion. The four linkers used were TAGLN4 (5′-AAAAAAAAAAC GCTATGAGTGTCTTGCC-pur), TAGLN8 (5′-AAAAAAAAAACTTGG TGTGTGTCTTGCC-pur), TAGLN9 (5′-AAAAAAAAAACGCTCGCTA TGAGTGTCC-pur), and TAGLN16 (5′-AAAAAAAAAAATGACGCTC TTGGTGTCC-pur) and were prepared with an automated DNA synthesizer (PE BioSystems Expedite 8909) using conventional phosphoramidite chemistry and reagents from Glen Research.

Four amino-modified DNA capture probes that were complementary to 16 nucleotides of the TAGLN linkers were synthesized: TAGCP4 (5′-CAAGACACTCATAGCG-3′), TAGCP8 (5′-CAAGACA CACACCAAG-3′), TAGCP9 (5′-ACACTCATAGCGAGCG-3′), and TAGCP16 (5′-ACACCAAGAGCGTCAT-3′). The 500 μM capture oligonucleotides in 50 mM sodium carbonate (pH 9) were spotted onto an amine-reactive glass surface with a 3-axis robot (MicroGrid,

BioRobotics), resulting in 200 μm features with 600 μm pitch. Each subgrid contained 24 spots of a single capture probe.

The mRNA-Fn3 fusion was prepared as described under Library Construction, except that the TAGLN series of puromycin-containing linkers was used. The fusion that contained the Fn3 variant T09.12, which binds TNF-α, was ligated to TAG8LN; the fusion that contained L09.20, which binds leptin, was ligated to TAG4LN; and the fusion that contained wild-type ^{10}Fn3 was ligated to TAG16LN. The RNA portion of the fusion was removed using RNase A (NEB). A mixture of the resulting constructs, which contained the encoding DNA oligonucleotide-puromycin linkers and the Fn3 proteins, was applied to the microarray for 16 hr at room temperature. The hybridized slide was washed in SSC and the slide was air-dried, then blocked with TBS, 0.05% Tween-20, 2% BSA.

To test the immobilized antibody mimics for target binding, recombinant target (TNF-α or leptin; PeproTech) was biotinylated with EZ-Link NHS-LC-LC (Pierce) and dialyzed against PBS. MALDI-TOF of the resulting conjugates confirmed that most of the target molecules had been modified with a single biotin molecule. 100 nM of a specific target in TBS, 0.05% Tween-20, 0.2% BSA was applied to the surface of the microarray for 2 hr; next, the slide was washed with TBS, 0.05% Tween-20. Cy3-labeled anti-biotin monoclonal antibody (Sigma) was applied to the microarray for 1 hr, and then the array was washed with TBS, 0.05% Tween. The slide was allowed to air-dry. Fluorescence laser scanning was performed with a GSI Lumonics ScasnArray 5000 system using 10 μm pixel resolution (Figure 5).

Acknowledgments

We thank Jack Szostak, Brian Seed, Gerald Joyce, Martin Wright, Ricky Baggio, and Ed Fritsch for stimulating discussion and the rest of Phylos, Inc., for their support.

Received: February 11, 2002
Revised: May 15, 2002
Accepted: July 17, 2002

References

1. Roberts, R.W., and Szostak, J.W. (1997). RNA-peptide fusions for the in vitro selection of peptides and proteins. Proc. Natl. Acad. Sci. USA *94*, 12297–12302.
2. Nemoto, N., Miyamoto-Sato, E., Husimi, Y., and Yanagawa, H. (1997). In vitro virus: bonding of mRNA bearing puromycin at the 3′-terminal end to the C-terminal end of its encoded protein on the ribosome in vitro. FEBS Lett. *414*, 405–408.
3. Roberts, R.W. (1999). Totally in vitro protein selection using mRNA-protein fusions and ribosome display. Curr. Opin. Chem. Biol. *3*, 268–273.
4. Liu, R., Barrick, J.E., Szostak, J.W., and Roberts, R.W. (2000). Optimized synthesis of RNA-protein fusions for in vitro protein selection. Methods Enzymol. *318*, 268–293.
5. Cho, G., Keefe, A.D., Liu, R., Wilson, D.S., and Szostak, J.W. (2000). Constructing high complexity synthetic libraries of long ORFs using in vitro selection. J. Mol. Biol. *297*, 309–319.
6. Keefe, A.D., and Szostak, J.W. (2001). Functional proteins from a random-sequence library. Nature *410*, 715–718.
7. Wilson, D.S., Keefe, A.D., and Szostak, J.W. (2001). The use of mRNA display to select high-affinity protein-binding peptides. Proc. Natl. Acad. Sci. USA *98*, 3750–3755.
8. Barrick, J.E., Takahashi, T.T., Balakin, A., and Roberts, R.W. (2001). Selection of RNA-binding peptides using mRNA-peptide fusions. Methods *23*, 287–293.
9. Mattheakis, L.C., Bhatt, R.R., and Dower, W.J. (1994). An in vitro polysome display system for identifying ligands from very large peptide libraries. Proc. Natl. Acad. Sci. USA *91*, 9022–9026.
10. Hanes, J., and Pluckthun, A. (1997). In vitro selection and evolution of functional proteins by using ribosome display. Proc. Natl. Acad. Sci. USA *94*, 4937–4942.
11. Hanes, J., Schaffitzel, C., Knappik, A., and Pluckthun, A. (2000). Picomolar affinity antibodies from a fully synthetic naive library selected and evolved by ribosome display. Nat. Biotechnol. *18*, 1287–1292.
12. Sidhu, S.S., Lowman, H.B., Cunningham, B.C., and Wells, J.A. (2000). Phage display for selection of novel binding peptides. Methods Enzymol. *328*, 333–363.
13. Koehler, G., and Milstein, C. (1975). Continuous cultures of fused cells secreting antibody of predefined specificity. Nature *256*, 495–497.
14. Clackson, T., Hoogenboom, H.R., Griffiths, A.D., and Winter, G. (1991). Making antibody fragments using phage display libraries. Nature *352*, 624–628.
15. Marks, J.D., Hoogenboom, H.R., Bonnert, T.P., McCafferty, J., Griffiths, A.D., and Winter, G. (1991). By-passing immunization. Human antibodies from V-gene libraries displayed on phage. J. Mol. Biol. *222*, 581–597.
16. Barbas, C.F.d., Bain, J.D., Hoekstra, D.M., and Lerner, R.A. Semisynthetic combinatorial antibody libraries: a chemical solution to the diversity problem. (1992). Proc. Natl. Acad. Sci. USA *89*, 4457–4461.
17. Akamatsu, Y., Cole, M.S., Tso, J.Y., and Tsurushita, N. (1993). Construction of a human Ig combinatorial library from genomic V segments and synthetic CDR3 fragments. J. Immunol. *151*, 4651–4659.
18. Hoogenboom, H.R., Griffiths, A.D., Johnson, K.S., Chiswell, D.J., Hudson, P., and Winter, G. (1991). Multi-subunit proteins on the surface of filamentous phage: methodologies for displaying antibody (Fab) heavy and light chains. Nucleic Acids Res. *19*, 4133–4137.
19. Chen, Y., Weismann, C., Fuh, G., Li, B., Christinger, H.W., McKay, P., de Vos, A.M., and Lowman, H.B. (1999). Selection and analysis of an optimized anti-VEGF antibody: crystal structure of an affinity-matured Fab in complex with antigen. J. Mol. Biol. *293*, 865–881.
20. de Haard, H.J., van Neer, N., Reurs, A., Hufton, S.E., Roovers, R.C., Henderikx, P., de Bruine, A.P., Arends, J.W., and Hoogenboom, H.R. (1999). A large non-immunized human Fab fragment phage library that permits rapid isolation and kinetic analysis of high affinity antibodies. J. Biol. Chem. *274*, 18218–18230.
21. Osterroth, F., Alkan, O., Mackensen, A., Lindemann, A., Fisch, P., Skerra, A., and Veelken, H. (1999). Rapid expression cloning of human immunoglobulin Fab fragments for the analysis of antigen specificity of B cell lymphomas and anti-idiotype lymphoma vaccination. J. Immunol. Methods *229*, 141–153.
22. Sheets, M.D., Amersdorfer, P., Finnern, R., Sargent, P., Lindquist, P., Schier, R., Hemingsen, G., Wong, C., Gerhart, J.C., Marks, J.D., et al. (1998). Efficient construction of a large nonimmune phage antibody library: the production of high-affinity human single-chain antibodies to protein antigens. Proc. Natl. Acad. Sci. USA *95*, 6157–6162.
23. Klimka, A., Matthey, B., Roovers, R.C., Barth, S., Arends, J.W., Engert, A., and Hoogenboom, H.R. (2000). Human anti-CD30 recombinant antibodies by guided phage antibody selection using cell panning. Br. J. Cancer *83*, 252–260.
24. Arndt, K.M., Muller, K.M., and Pluckthun, A. (2001). Helix-stabilized Fv (hsFv) antibody fragments: substituting the constant domains of a Fab fragment for a heterodimeric coiled-coil domain. J. Mol. Biol. *312*, 221–228.
25. Hamers-Casterman, C., Atarhouch, T., Muyldermans, S., Robinson, G., Hamers, C., Songa, E.B., Bendahman, N., and Hamers, R. (1993). Naturally occurring antibodies devoid of light chains. Nature *363*, 446–448.
26. Muyldermans, S., Atarhouch, T., Saldanha, J., Barbosa, J.A., and Hamers, R. (1994). Sequence and structure of VH domain from naturally occurring camel heavy chain immunoglobulins lacking light chains. Protein Eng. *7*, 1129–1135.
27. Martin, F., Volpari, C., Steinkuhler, C., Dimasi, N., Brunetti, M., Biasiol, G., Altamura, S., Cortese, R., De Francesco, R., and Sollazzo, M. (1997). Affinity selection of a camelized V(H) domain antibody inhibitor of hepatitis C virus NS3 protease. Protein Eng. *10*, 607–614.
28. Reiter, Y., Schuck, P., Boyd, L.F., and Plaksin, D. (1999). An antibody single-domain phage display library of a native heavy chain variable region: isolation of functional single-domain VH molecules with a unique interface. J. Mol. Biol. *290*, 685–698.
29. Riechmann, L., and Muyldermans, S. (1999). Single domain anti-

bodies: comparison of camel VH and camelised human VH domains. J. Immunol. Methods *231*, 25–38.
30. Conrath, K.E., Lauwereys, M., Galleni, M., Matagne, A., Frere, J.M., Kinne, J., Wyns, L., and Muyldermans, S. (2001). beta-lactamase inhibitors derived from single-domain antibody fragments elicited in the camelidae. Antimicrob. Agents Chemother. *45*, 2807–2812.
31. Desmyter, A., Decanniere, K., Muyldermans, S., and Wyns, L. (2001). Antigen specificity and high affinity binding provided by one single loop of a camel single-domain antibody. J. Biol. Chem. *276*, 26285–26290.
32. Muyldermans, S. (2001). Single domain camel antibodies: current status. J. Biotechnol. *74*, 277–302.
33. Muyldermans, S., Cambillau, C., and Wyns, L. (2001). Recognition of antigens by single-domain antibody fragments: the superfluous luxury of paired domains. Trends Biochem. Sci. *26*, 230–235.
34. Ohage, E., and Steipe, B. (1999). Intrabody construction and expression. I. The critical role of VL domain stability. J. Mol. Biol. *291*, 1119–1128.
35. Dubnovitsky, A.P., Kravchuk, Z.I., Chumanevich, A.A., Cozzi, A., Arosio, P., and Martsev, S.P. (2000). Expression, refolding, and ferritin-binding activity of the isolated VL-domain of monoclonal antibody F11. Biochemistry *65*, 1011–1018.
36. van den Beucken, T., van Neer, M., Sablon, E., Desmet, J., Celis, L., Hoogenboom, H.R., and Hufton, S.E. (2001). Building novel binding ligands to B7.1 and B7.2 based on human antibody single variable light chain domains. J. Mol. Biol. *310*, 591–601.
37. Williams, W.V., Kieber-Emmons, T., VonFeldt, J., and Greene, M.I. (1991). Design of bioactive peptides based on antibody hypervariable region structures. Development of conformationally constrained and dimeric peptides with enhanced affinity. J. Biol. Chem. *266*, 5182–5190.
38. Monfardini, C., Kieber-Emmons, T., Vost, D., Godillot, A.P., Weiner, D.B., and Williams, W.V. (1996). Rational design of granulocyte-macrophage colony-stimulating factor antagonist peptides. J. Biol. Chem. *271*, 2966–2971.
39. Wang, B., Yang, H., Liu, Y.C., Jelinek, T., Zhang, L., Ruoslahti, E., and Fu, H. (1999). Isolation of high-affinity peptide antagonists of 14-3-3 proteins by phage display. Biochemistry *38*, 12499–12504.
40. Arndt, K.M., Pelletier, J.N., Muller, K.M., Alber, T., Michnick, S.W., and Pluckthun, A. (2000). A heterodimeric coiled-coil peptide pair selected in vivo from a designed library-versus-library ensemble. J. Mol. Biol. *295*, 627–639.
41. Sperinde, J.J., Choi, S.J., and Szoka, F.C., Jr. (2001). Phage display selection of a peptide DNase II inhibitor that enhances gene delivery. J. Gene Med. *3*, 101–108.
42. Noren, K.A., and Noren, C.J. (2001). Construction of high-complexity combinatorial phage display peptide libraries. Methods *23*, 169–178.
43. Tramontano, A., Bianchi, E., Venturini, S., Martin, F., and Pessi, A. (1994). The making of the minibody: an engineered b-protein for the display of conformationally constrained peptides. J. Mol. Recognit. *7*, 9–24.
44. McConnell, S., and Hoess, R. (1995). Tendamistat as a scaffold for conformationally constrained phage peptide libraries. J. Mol. Biol. *250*, 460–470.
45. Braisted, A.C., and Wells, J.A. (1996). Minimizing a binding domain from protein A. Proc. Natl. Acad. Sci. USA *93*, 5688–5692.
46. Abedi, M.R., Caponigro, G., and Kamb, A. (1998). Green fluorescent protein as a scaffold for intracellular presentation of peptides. Nucleic Acids Res. *26*, 623–630.
47. Martin, F., Dimasi, N., Volpari, C., Perrera, C., Di Marco, S., Brunetti, M., Steinkuhler, C., De Francesco, R., and Sollazzo, M. (1998). Design of selective eglin inhibitors of HCV NS3 proteinase. Biochemistry *37*, 11459–11468.
48. Beste, G., Schmidt, F.S., Stibora, T., and Skerra, A. (1999). Small antibody-like proteins with prescribed ligand specificities derived from the lipocalin fold. Proc. Natl. Acad. Sci. USA *96*, 1898–1903.
49. Nuttall, S.D., Rousch, M.J., Irving, R.A., Hufton, S.E., Hoogenboom, H.R., and Hudson, P.J. (1999). Design and expression of soluble CTLA-4 variable domain as a scaffold for the display of functional polypeptides. Proteins *36*, 217–227.
50. Gunneriusson, E., Nord, K., Uhlen, M., and Nygren, P. (1999). Affinity maturation of a Taq DNA polymerase specific affibody by helix shuffling. Protein Eng. *12*, 873–878.
51. Shusta, E.V., Holler, P.D., Kieke, M.C., Kranz, D.M., and Wittrup, K.D. (2000). Directed evolution of a stable scaffold for T-cell receptor engineering. Nat. Biotechnol. *18*, 754–759.
52. Skerra, A. (2001). 'Anticalins': a new class of engineered ligand-binding proteins with antibody-like properties. J. Biotechnol. *74*, 257–275.
53. Nord, K., Nord, O., Uhlen, M., Kelley, B., Ljungqvist, C., and Nygren, P.A. (2001). Recombinant human factor VIII-specific affinity ligands selected from phage-displayed combinatorial libraries of protein A. Eur. J. Biochem. *268*, 4269–4277.
54. Bork, P., and Doolittle, R.F. (1992). Proposed acquisition of an animal protein domain by bacteria. Proc. Natl. Acad. Sci. USA *89*, 8990–8994.
55. Little, E., Bork, P., and Doolittle, R.F. (1994). Tracing the spread of fibronectin type III domains in bacterial glycohydrolases. J. Mol. Evol. *39*, 631–643.
56. Main, A.L., Harvey, T.S., Baron, M., Boyd, J., and Campbell, I.D. (1992). The three-dimensional structure of the tenth type III module of fibronectin: an insight into RGD-mediated interactions. Cell *71*, 671–678.
57. Dickinson, C.D., Veerapandian, B., Dai, X.P., Hamlin, R.C., Xuong, N.H., Ruoslahti, E., and Ely, K.R. (1994). Crystal structure of the tenth type III cell adhesion module of human fibronectin. J. Mol. Biol. *236*, 1079–1092.
58. Leahy, D.J., Erickson, H.P., Aukhil, I., Joshi, P., and Hendrickson, W.A. (1994). Crystallization of a fragment of human fibronectin: introduction of methionine by site-directed mutagenesis to allow phasing via selenomethionine. Proteins *19*, 48–54.
59. Leahy, D.J., Aukhil, I., and Erickson, H.P. (1996). 2.0 Å crystal structure of a four-domain segment of human fibronectin encompassing the RGD loop and synergy region. Cell *84*, 155–164.
60. Plaxco, K.W., Spitzfaden, C., Campbell, I.D., and Dobson, C.M. (1996). Rapid refolding of a proline-rich all-beta-sheet fibronectin type III module. Proc. Natl. Acad. Sci. USA *93*, 10703–10706.
61. Koide, A., Jordan, M.R., Horner, S.R., Batori, V., and Koide, S. (2001). Stabilization of a fibronectin type III domain by the removal of unfavorable electrostatic interactions on the protein surface. Biochemistry *40*, 10326–10333.
62. Koide, A., Bailey, C.W., Huang, X., and Koide, S. (1998). The fibronectin type III domain as a scaffold for novel binding proteins. J. Mol. Biol. *284*, 1141–1151.
63. Skerra, A. (2000). Engineered protein scaffolds for molecular recognition. J. Mol. Recognit. *13*, 167–187.
64. Cadwell, R.C., and Joyce, G.F. (1992). Randomization of genes by PCR mutagenesis. PCR Methods Appl. *2*, 28–33.
65. Weng, S., Gu, K., Hammond, P.W., Lohse, P., Rise, C., Wagner, R.W., Wright, M.C., and Kuimelis, R.G. (2002). Generating addressable protein microarrays with PROfusion covalent mRNA-protein fusion technology. Proteomics *2*, 48–57.
66. Schaffitzel, C., Berger, I., Postberg, J., Hanes, J., Lipps, H.J., and Pluckthun, A. (2001). In vitro generated antibodies specific for telomeric guanine-quadruplex DNA react with *Stylonychia lemnae* macronuclei. Proc. Natl. Acad. Sci. USA *98*, 8572–8577.
67. Silzel, J.W., Cerek, B., Dodson, C., Tsay, T., and Obremski, R.J. (1998). Mass-sensing, multianalyte microarray immunoassay with imaging detection. Clin. Chem. *44*, 2036–2043.
68. Mendoza, L.G., McQuary, P., Mongan, A., Gangadharan, R., Brignac, S., and Eggers, M. (1999). High-throughput microarray-based enzyme-linked immunosorbent assay (ELISA). Biotechniques *27*, 778–788.
69. MacBeath, G., and Schreiber, S.L. (2000). Printing proteins as microarrays for high-throughput function determination. Science *289*, 1760–1763.
70. Spinelli, S., Frenken, L., Bourgeois, D., de Ron, L., Bos, W., Verrips, T., Anguille, C., Cambillau, C., and Tegoni, M. (1996). The crystal structure of a llama heavy chain variable domain. Nat. Struct. Biol. *3*, 752–757.